FINITE ELEMENT MODELING OF PRESTRESSED GIRDER STRENGTHENING USING FIBER REINFORCED POLYMER AND CODAL COMPARISON

by

MURUGANANDAM MOHANAMURTHY

Presented to the Faculty of the Graduate School of
The University of Texas at Arlington in Partial Fulfillment
of the Requirements
for the Degree of

MASTER OF SCIENCE IN CIVIL ENGINEERING

THE UNIVERSITY OF TEXAS AT ARLINGTON

December 2013

Acknowledgements

I thank Dr. Nur Yazdani for his constant support and guidance throughout the past two years. I thank him for bearing with my faults and guiding me and helping me achieve the confidence to present my research. I thank him for his constant criticism which has given me a positive outlook towards the various problems faced during my research and strengthened my determination and confidence, without which I will not be in the position where I am right now.

I would like to express my deepest gratitude to my committee members Dr. Mohammad Najafi and Dr. Shih Ho-Chao for their constant support and encouragement. I would like to thank my friends, roommates and class mates for their support, encouragement and critics.

I take this opportunity to thank my parents, and my sister for being so lovable and kind.

November 21, 2013

Abstract

FINITE ELEMENT MODELING OF PRESTRESSED GIRDER STRENGTHENING USING FIBER REINFORCED POLYMER AND CODAL COMPARISON

MURUGANANDAM MOHANAMURTHY, MS

The University of Texas at Arlington, 2013

Supervising Professor: Nur Yazdani

Fiber Reinforced Polymer (FRP) composite materials provide effective and potentially economic solution for rehabilitating and upgrading the existing reinforced and precast concrete bridge structures that have suffered deterioration. Each year, there are a significant number of damaged bridges, mainly due to reinforcing steel corrosion, structural failure or vehicle collision. Using FRP materials has many advantages over other strengthening methods. This study consists of reviewing relevant guidelines, codes, standard practices and manufacturer's specifications that deals with FRP strengthening of damaged concrete bridges based on both U.S and international sources. Based on literature review, the available design guidelines are summarized and compared. Comparison includes flexural load carrying capacity of prestressed girder and failure mode based on reviewed code provisions for an experimental model and results validated with finite element analysis. Design code recommendations are made based on the comparative study.

Table of Contents

List of Illustrations

List of Tables

Chapter 1

Introduction

America's infrastructure report states that over 11% of the nation's 607,380 bridges are structurally deficient and an estimated $20.5 billion is required annually to upgrade the nation's deficient bridges by the year 2028 ("Report Card on America's Infrastructure," 2013). However, the current annual expenditure for bridge investments is only $12.8 billion and an additional $8 billion is required annually to upgrade the nation's deficient bridges ("Report Card on America's Infrastructure," 2013).

Bridge retrofitting may reduce budget constraints and construction time. The highway department in each state handles a considerable number of bridges that are damaged due to vehicle or vessel collision, reinforcing steel corrosion or fire each year. Fiber Reinforced Polymer (FRP) strengthening method is the most popular and best method to repair damaged bridges since 1999 (Yang, Merrill, & Bradberry, 2011). FRP wrapping improves flexural, shear, axial, and torsional strengths, and also serviceability of existing or damaged bridges.

FRP is a composite material manufactured in the form of polymer matrix reinforced with fibers. Common available fibers are glass, carbon, or aramid, and polymers made up of epoxy, vinyl ester or polyester. FRP composite wrapping is a highly promising structural strengthening process and has been successfully used for the strengthening of structures. FRP wrapping has more advantages than adding reinforcement or steel plates to increase the strength of structures; it is lighter in weight, non-corrosive in nature and has a significant load capacity. The installation of FRP laminates is faster, simpler and less labor intensive, compared to adding structural steel or casting additional reinforced concrete. Use of FRP wrapping for in-service bridge

repair or strengthening is economic, where prolonged construction time may lead to transportation difficulties.

The U.S Department of Transportation (USDOT) has published the number of structurally deficient (SD) bridges and the number of replaced bridges by state ("U.S department of transportation federal highway administration," 2012). FRP strengthening can save or increase the life of a bridge and reduce the cost for replacement. USDOT has estimated that $35 billion is required for rehabilitation of such bridges. About 11% of all U.S. bridges are classified as SD, as shown in the table 1-1 by state ("U.S department of transportation federal highway administration," 2012).

Table 1-1 U.S. States, Ranked by Percentage of Deficient National Highway System and Non-National Highway System Bridges (USDOT)

State	Total Number of SD NHS and NNHS Bridges	Total Area (m^2) of SD NHS and NNHS Bridges	Total Number of SD NHS and NNHS Bridges Replaced in 2012	Total Area (m^2) of SD NHS and NNHS Bridges Replaced in 2012
AK	128	68,823	3	2,937
AL	1448	342,546	13	21,439
AR	898	348,220	15	29,489
AZ	247	216,443	8	21,951
CA	2978	4,430,018	11	8,396
CO	566	268,894	11	13,460
CT	406	548,027	12	8,105
DC	30	97,552	0	0
DE	53	40,448	1	71
FL	262	469,031	8	37,002
GA	878	301,543	21	28,591
HI	146	45,228	1	1,434
IA	5193	934,995	45	21,815
ID	397	128,013	9	10,092
IL	2311	1,269,106	84	50,617
IN	2036	767,158	22	9,351
KS	2658	401,519	7	5,099

Table 1-1—*Continued*

KY	1244	427,192	20	19,781
LA	1783	1,554,626	51	34,960
MA	493	611,797	14	8,824
MD	368	238,114	8	6,516
ME	356	141,348	7	8,736
MI	1354	567,606	42	17,497
MN	1190	378,634	15	6,624
MO	3528	1,133,467	97	40,560
MS	2417	557,171	32	34,243
MT	399	134,292	5	2,647
NC	2192	904,938	100	71,481
ND	746	91,397	2	860
NE	2779	349,565	22	25,815
NH	362	121,801	0	0
NJ	651	705,774	6	3,748
NM	307	124,858	9	7,259
NV	40	15,713	0	0
NY	2169	1,781,400	29	13,537
OH	2462	993,235	47	35,337
OK	5382	1,138,086	79	59,301
OR	433	251,413	11	3,133
PA	5540	1,961,846	118	76,124
PR	282	228,611	4	2,224
RI	156	173,760	6	2,841
SC	1141	558,579	8	31,878
SD	1208	193,144	8	4,333
TN	1195	501,054	13	29,801

1.1 FRP Flexural Strengthening Sequence

Figure 1-1 shows a bridge girder damaged due to vehicle collision. It is possible to see the damaged reinforcement in the girder. Detailed structural analysis is required to determine the feasibility of FRP strengthening based on the number of usable strands and their condition.

Figure 1-1 Damaged Concrete Girder

(Image: Courtesy Texas Department of Transportation (TXDOT))

Figure 1-2 shows the damaged girder after the removal of loose concrete and debris. Wire mesh netting is provided around the girder to temporarily contain debris on the girder.

Figure 1-2 Wire Netting on the Bottom of Damaged Girder

(Image: Courtesy TXDOT)

Figure 1-3 shows spliced strands provided at a design lap length. All the damaged strands are straightened and spliced with a bar of equal diameter using a mechanical splice device. All damaged strands are spliced and prestressed to meet the design strength criteria.

Figure 1-3 Spliced Strands

(Image: Courtesy TXDOT)

Figure 1-4 shows recasting of the damaged portion by using plywood material as formwork. Cast in place concrete is used for this purpose. The old concrete surface should be chipped to ensure perfect bonding between fresh concrete and existing concrete structure before recasting the damaged portion.

Figure 1-4 Form Work

(Image: Courtesy TXDOT)

Figure 1-5 & 1-6 shows recasting of concrete and compacting to attain original shape of girder.

Figure 1-5 Casting Concrete

(Image: Courtesy TXDOT)

Figure 1-6 Consolidation

(Image: Courtesy TXDOT)

Figure 1-7 shows the repaired girder after removal of form work. It is now ready for the application of FRP layers.

Figure 1-7 Finished Surface

(Image: Courtesy TXDOT)

Figure 1-8 FRP Wrapping

(Image: Courtesy USDOT)

Figure 1-8 shows the FRP layer applied to the damaged prestressed girder. In first step surface primer is applied using nap roller and then putty applied to eliminate uneven surfaces. After that, first layer of resin is applied to prepared surface using nap roller. Next step, proper width and length dry fabric fiber is applied on the surface using rib roller. Above that second layer of resin is applied to enclose fibers. Additional layers can be added using the same procedure.

1.2 State Highway Survey

We conducted an E-mail survey of the state highway departments in the United States to find the various concrete bridge retrofitting techniques that they are using. Based on the E-mail survey and internet source it was discovered that 24 departments are using FRP laminate application as a bridge retrofitting technique. The corresponding states are: Alabama, California, Colorado, Florida, Hawaii, Idaho, Indiana, Iowa, Kansas,

Louisiana, Michigan, Missouri, Nebraska, Nevada, New Jersey, New Mexico, New York, North Carolina, Oregon, Pennsylvania, South Dakota, Texas, Washington, Wisconsin.

1.3 Research Significance

While there are several available design guides, standards and manufacture's guidelines for FRP strengthening of concrete structures, the ultimate utilization FRP material properties and research in this area are limited. Research and improvement in this field will be helpful for infrastructure development, especially in bridge strengthening. Due to the changes in traffic volume and modern vehicle design and loads, most bridges need to be upgraded to carry the additional load. Another issue in recent days is over height vehicles collisions due to low clearance of older bridges or increase of roadway overlay thickness. Research in this field will contribute to the nation's infrastructure growth and economy.

1.4 Objective of the Study

The objective of this study is to find an effective design procedure for FRP strengthening of damaged prestressed concrete bridge girder, and to investigate the accuracy of flexural load capacity, crack pattern, and failure mode prediction using an available non-linear finite element computer program.

1.5 Overview of Research Program

This study involved the comparison of FRP wrap strengthening procedures from some of these available publications for concrete bridges. Comparison includes flexural load carrying capacity of prestressed girder and failure mode based on reviewed code provisions for an experimental model and results validated with finite element analysis. Design code recommendations are made based on the comparative study. Figure 1-19 shows the major milestones of the research performed in this study.

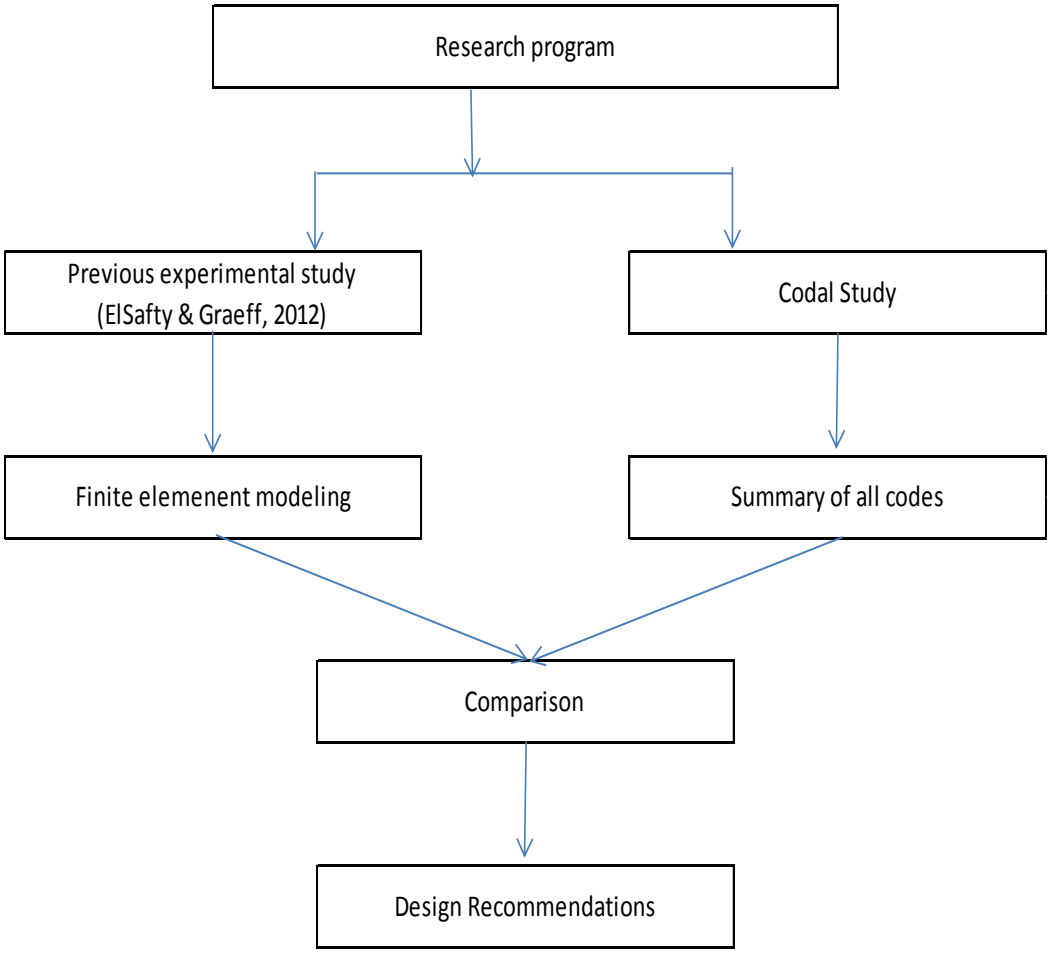

Figure 1-9 Diagramof Research Program

Chapter 2

Literature Review

2.1 Fiber Reinforced Polymer Application on Bridges

Over-height vehicles frequently collide with prestressed concrete and reinforced concrete bridge across the world (Miller, 2006). In last decade strengthening of beam achieved by adding additional beams using steel plates and it has many disadvantages (Tedesco, Stallings, & EL-Mihilmy, 1998). In recent days FRP strengthening method followed by many DOT's and it gives economical solution (GangaRao & Vijay, 1998). Even though, there are no well-developed design codes and specifications for the use of FRP for strengthening and number of agencies and institutions developing these documents across the nation (Gilstrap, Burke, Dowden, & Dolan, 1997). The development includes experimental investigation and analytical investigation that helps to come effective design guidelines. Recent development in finite element software can model strengthened prestressed concrete bridge girder by providing Initial pre-stress, self-weigh, and also initial crack, zero deflection point, yielding of steel, decompression, flexural failure can predict from that (Wolanski, 2004).

2.2 Available Codes and Design Philosophy

Review of Current Practice

Several standards and guidelines for FRP strengthening of concrete structures from U.S and other countries were located after a through literature review and are listed below:

- ACI 440.2R-08, "Guide for the Design and Construction of Externally-Bonded FRP Systems for Strengthening Concrete Structures", (ACI, 2008).

- AASHTO 2012, “Guide Specifications for Design of Bonded FRP Systems for Repair and Strengthening of Concrete Bridge Elements”, (AASHTO, 2012).
- ISIS Canada Design Manual, 2001, “Strengthening Reinforced Concrete Structures with Externally-Bonded Fiber Reinforced Polymers”, (ISIS, 2001).
- FIB Technical Report Bulletin 14, “Externally Bonded FRP Reinforcement for RC Structures”, (FIB Bulletin 14, 2001).
- CNR 2004, “Guide for the Design and Construction of Externally Bonded FRP Systems for Strengthening Existing Structures – Materials, RC and PC Structures, Masonry Structures (CNR-DT 200, 2004).
- NCHRP Report 655, “Recommended Guide Specification for the Design of Externally Bonded FRP Systems for Repair and Strengthening of Concrete Bridge Elements”, (NCHRP Report 655, 2010).
- TR55, 2012, “Design Guidance for Strengthening Concrete Structures Using Fiber Composite Materials”, (TR55, 2012).

Initially, Some of the DOT’s used FRP manufacture’s guidelines to determine FRP system strengths, because there were no other existing codes. In 1998, the MBrace FRP strengthening design guide was developed by the BASF chemical company, and it has been used since then by some DOT’s. BASF recently discontinued the MBrace guide and currently recommends the ACI 440 guidelines. In 2001, FIB published a technical report on design and use of externally bonded FRP for reinforced concrete structures (FIB Bulletin 14, 2001). In 2002, ACI published the first edition of its FRP strengthening design guide; it was developed based on the MBrace guide (ACI, 2008). In 2008, ACI published the second edition of the FRP strengthening guide. Subsequently, other guides

were published in Canada (ISIS, 2001), Italy (CNR-DT 200, 2004). In U.K., the TR55 technical report on FRP strengthening was published first in 2000, with subsequent upgrades (TR55, 2012). AASHTO published the first edition of its guide specifications in 2012, based on NCHRP 655, and NCHRP 688 reports (AASHTO, 2012; NCHRP Report 655, 2010).

2.2.1 ACI 440 2R-08

In ACI 440, FRP strengthening design is based on ACI 318-05 strength and serviceability requirements. This guide recommends additional reduction factors which are applied to FRP laminate strength capacity. These reduction factor values were calculated based on experimental results and analytical simulations. The moment equation from this code is shown in Equation. 1. All parameters are defined in the "Notations" section in the latter part of this study.

Moment capacity (ACI 440 2R-08)

$$M_r = \Phi\left[A_{ps}f_{ps}\left(d_{ps} - \frac{\beta_1 c}{2}\right) + \Psi A_f f_{fe}\left(h - \frac{\beta_1 c}{2}\right)\right] \quad (1)$$

1. If εc is 0.003

β1 - Stress block factor specified in Article 10.2.7.3 of ACI 318-11.

2. If εc is less than 0.003

β1 – Stress block factor shall be calculated according to the following equation.

$$\beta_1 = \frac{4\varepsilon_c' - \varepsilon_c}{6\varepsilon_c' - 2\varepsilon_c}$$

2.2.2 AASHTO 2012

In AASHTO 2012, service, strength, and extreme event limit state combinations are considered as per AASHTO LRFD recommendations for FRP strengthening.The moment capacity from this code is presented in Equations 2 and 3:

Moment capacity (AASHTO)

1. If ε_c is 0.003

$$M_r = \Phi \left[A_{ps} f_{ps} \left(d_{ps} - \frac{\beta_1 c}{2}\right)\right] + \Phi_f T_f \left(h - \frac{\beta_1 c}{2}\right) \quad (2)$$

β1 – Stress block factor specified in Article 5.7.2.2 of AASHTO LRFD.

2. If ε_c is less than 0.003

$$M_r = \Phi \left[A_{ps} f_{ps} \left(d_{ps} - k_2 c\right)\right] + \Phi_f T_f \left(h - k_2 c\right) \quad (3)$$

In which:

$$T_f = b_{frb} N_b$$

$$k_2 = 1 - \frac{2\left[\left(\frac{\varepsilon_c}{\varepsilon_o}\right) - \tan^{-1}\left(\frac{\varepsilon_c}{\varepsilon_o}\right)\right]}{\beta_2 \left(\frac{\varepsilon_c}{\varepsilon_o}\right)^2}$$

$$\beta_1 = \frac{\mathrm{Ln}\left[1 + \left(\frac{\varepsilon_c}{\varepsilon_o}\right)^2\right]}{\left(\frac{\varepsilon_c}{\varepsilon_o}\right)}$$

2.2.3 FIB 14

In FIB 14, design calculations are based on analytical or empirical models. This design procedure is verifies both service limit state (SLS) and ultimate limit state method (ULS). In SLS stresses, creep, and deformations are verified and in ULS different type of failure modes are verified. The moment capacity from this code is presented in Equation. 4:

Moment capacity (FIB)

$$M_r = A_{ps} f_{ps} \left(d_{ps} - k_2 c\right) + A_f E_f \varepsilon_f (h - k_2 c) \quad (4)$$

In which:

$$k_2 = \begin{cases} \dfrac{8 - 1000\,\varepsilon_c}{4\,(6 - 1000\varepsilon_c)} & for\ \varepsilon_c \leq 0.002. \\ \dfrac{1000\varepsilon_c\,(3000\varepsilon_c - 4) + 2}{2000\,\varepsilon_c\,(3000\varepsilon_c - 2)} & for\ 0.002 \leq \varepsilon_c \leq 0.0035 \end{cases}$$

2.2.4 TR 55

In TR 55, design principles are based on limit state principle. In ultimate limit state design bending, shear, compression, and FRP ruptures are considered. In service limit state design deflection, concrete crack widths, and stress limitations are considered. The moment capacity from this code is presented in Equation 5.

Moment capacity (TR55)

$$M_r = M_{existing} + A_f \varepsilon_{fe} E_f \, z \tag{5}$$

In which:

ε_{fe} = Design strain value of FRP

z = Prestressed steel lever arm

2.2.5 CNR 2004

In CNR 2004, design of FRP strengthening is based on the strength and strain properties of FRP laminate. Partial factor and environmental reduction factors are considered in the design. The mo

ment capacity from this code is presented in Equation 6:

Moment capacity:

$$M_r = \frac{1}{\gamma_{Rd}} \left[\Psi \cdot b \cdot c \cdot f_{cd}\left(d_{ps} - \lambda \cdot c\right)\right] + A_f \cdot \sigma_f \cdot d_1 \tag{6}$$

2.2.6 ISIS Canada

In ISIS Canada, the initial strains in existing structures are usually assumed to be negligible and the stress and strain distribution values are approximated. The moment capacity from this publication is shown in Equation 7:

Moment capacity

$$M_r = \Phi \, f_{ps} A_{ps} \left(d_p - \frac{a}{2}\right) + \Phi_f E_f A_f \varepsilon_f \left(h - \frac{a}{2}\right) \tag{7}$$

In which:

$$\alpha_1 = 0.85 - 0.0015\, f_c' \geq 0.67$$

$$\beta_1 = 0.97 - 0.0025\, f_c' \geq 0.67$$

All the located guide procedures consider minimum requirements necessary to provide for public safety. Each publication specifies its own partial factor of safety, characteristic values of material properties, design values of material properties and strength reduction factor. It results in conservative design and does not allow the maximum utilization of material properties. For flexural design, most guidelines follow trial and error methods to predict the natural axis of the FRP strengthened structures, in the absence of any direct method. In AASHTO, the assumed maximum usable strain at the FRP/concrete interface is specified as 0.005; there is no such assumption made in the ACI or other codes. All the publications considered specify different interpolation methods to calculate the compression stress block parameters and may result in differences in calculated strengths. The TR55 considers maximum FRP strain of 0.008; if this limit is exceeded, the publications states that the strengthened structure may fail due to separation of the FRP.

Chapter 3

Previous Experimental Study

A half scale FRP flexural repaired AASTHO prestressed concrete girder type II was previously tested at the University of North Florida (ElSafty & Graeff, 2012). The girder was 20 ft. long and an average concrete compressive strength of approximately 10 ksi was used. A total of five low-relaxation grade 270 seven-wire prestressing strands and three non-prestressed rebars were provided in the girder. An additional 4 in. thick decking with two rebars was cast on top to simulate a composite section. Figure 3-1 shows the cross-section and the reinforcement details.

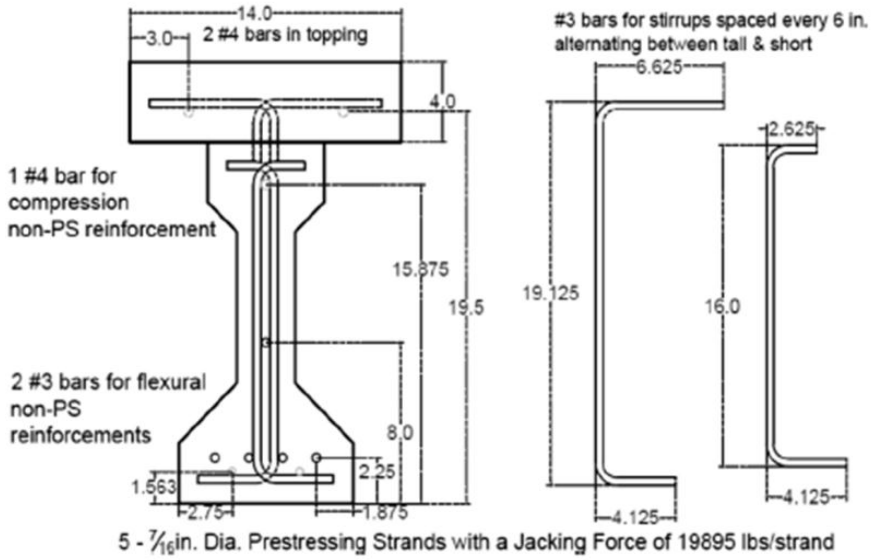

Figure 3-1 Prestressed Girder Cross-Section (ElSafty & Graeff, 2012)

The lateral damage was simulated by making a cut approximately 1 inch wide through the bottom flange of the girder and one of the prestressing strands using a saw. To improve the bonding of the repair materials, the cut and the surfaces around it were roughened using a chisel. Any loose materials and dust were removed from the cut using a water jet or pressurized air. A high-pressure epoxy injection procedure was performed

on the cut using a high-strength cementations mortar to achieve a near-perfect concrete cross-section. It is shown in figure in 3-2.

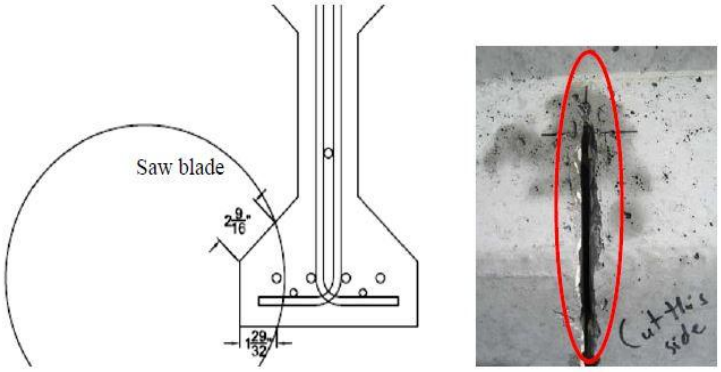

Figure 3-2 Damaged Girder (ElSafty & Graeff, 2012)

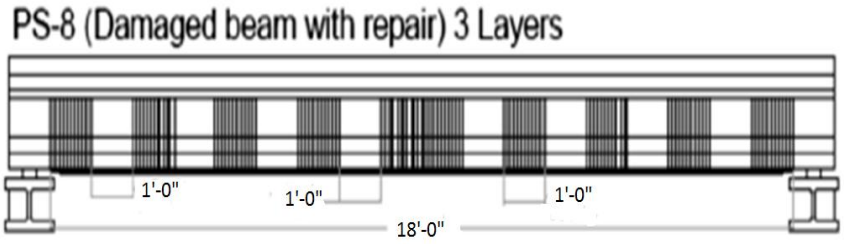

Figure 3-3 Prestressed Girder with FRP Layer (ElSafty & Graeff, 2012)

Figure 3-2 shows the CFRP layer arrangement used in the study. Three layers of longitudinal CFRP 17 ft. in length were provided at the bottom of the girder. For transverse U-wrapping, 12 in wide CFRP strips were used that extended up to the girder web as shown.

Tables 3-1 and 3-2 present the material properties used in the experiments. Typical dry fiber properties values given are based on ASTM test result, composite gross laminate properties are design properties of FRP based on ACI 440 suggestion.

Table 3-1 Properties of CFRP Materials (ElSafty & Graeff, 2012)

CFRP Material Properties	Typical Dry Fiber Properties	*Composite Gross Laminate Properties
Tensile Strength	550 ksi (3.79 GPa)	121 ksi (834 MPa)
Tensile Modulus	33.4 x 10^6 psi (234 GPa)	11.9 x 10^6 psi (82 GPa)
Ultimate Elongation	1.70%	0.85%
Density	0.063 lb/in^3 (1.74 g/cm^3)	N/A
Weight per sq. yd.	19oz. (644 g/m^2)	N/A
Rupture strain	0.012	0.012
Nominal Thickness	N/A	0.04 in. (1.0 mm)
*Gross laminate design properties based on ACI 440 suggested guidelines will vary slightly		

Table 3-2 Properties of Steel Reinforcements (ElSafty & Graeff, 2012)

Steel reinforcements	Prestressing Strands	#3 mild steel rebar	#4 mild steel rebar
Diameter	0.4375 in. (11.1mm)	0.375 in. (9.53 mm)	0.5 in (12.7 mm)
Steel area	0.115 in^2 (96.9 mm^2)	0.11 in^2(71.3 mm^2)	0.2 in^2(126 mm^2)
Steel Grade	270	60	60
Young's mod.	27.5 x 10^3 ksi	29 x 10^3 ksi	29 x 10^3 ksi
Weight	0.367 lb/ft	0.376 lb/ft	0.683 lb/ft
Yield Strength	243 ksi (1676 MPa)	60 ksi (345 N/mm^2)	60 ksi (345 N/mm^2)
Ult. Strength	270 ksi (1862 MPa)	90 ksi (621 N/mm^2)	90 ksi (621 N/mm^2)

3.1 Test Setup

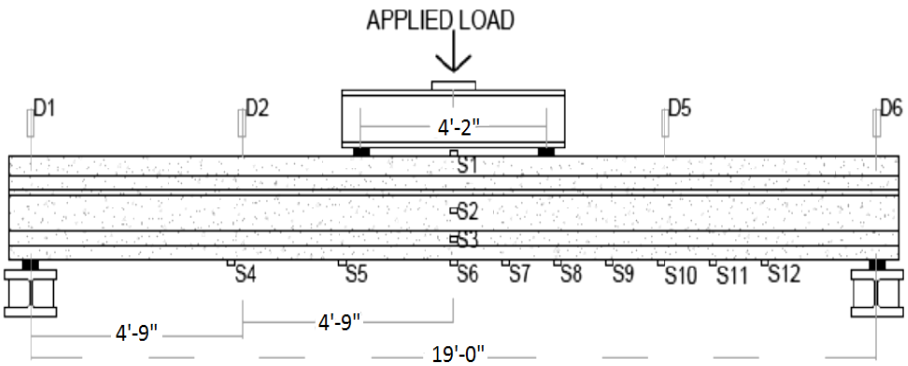

Figure 3-4 Test Setup

Figure 3-4 shows the test setup used in the experiment. The half-scale PS girders were statically tested by arranging the 20 ft long girders spanned across 19 ft and resting them on neoprene pads. A steel I-beam spreader bar was positioned at the mid-span of the beam and rested on two neoprene bearing pads with a center to center distance of 4 feet 2 inch. The load to the top surface of the spreader beam was measured using an actuator. LVDT deflection gauges were set-up at the middle of the span above and below the beam. LVDT deflection gauges (D_x) were also placed over both the supports and the quarter points in the beam. Twelve Strain gauges (S_x) were used along the cross-section height and the tension face of the beam.

Chapter 4

Finite Element Modeling

ANSYS Parametric Design Language (APDL) 14.5 was used to model damaged prestressed girder. It is capable of predicting FRP strengthened prestressed girder non-linear behavior.

4.1 Element Type

SOLID65 is an element used to create 3-D models of concrete. This element is capable of simulating concrete cracking in tension and concrete crushing in compression. Figure 4-1 shows the element and node arrangement. It has eight nodes and three degrees of freedom at each node.

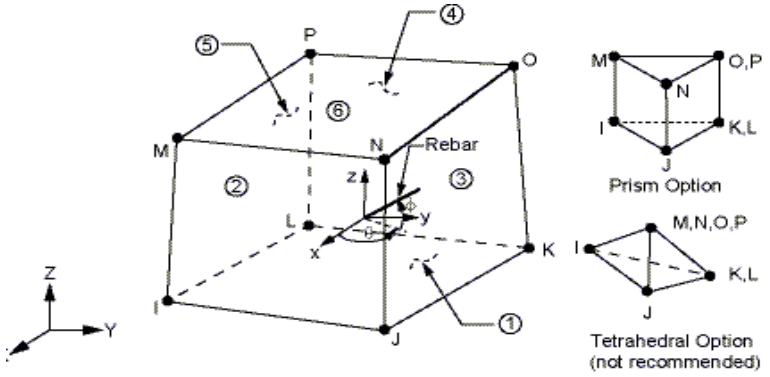

Figure 4-1 Solid65 Geometry (ANSYS, 2012)

LINK180 element was used to model rebars and prestressed bars. Figure 4-2 shows link element node arrangement. It has two nodes with three degree of freedom in each node.

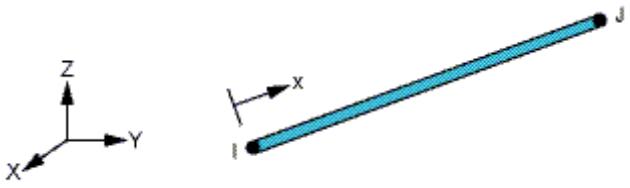

Figure 4-2 Link180 Geometry (ANSYS, 2012)

The SHELL41 element was used to model FRP layer. Figure 4-3 shows the shell41 element. It has four nodes and each node has three degrees of freedom.

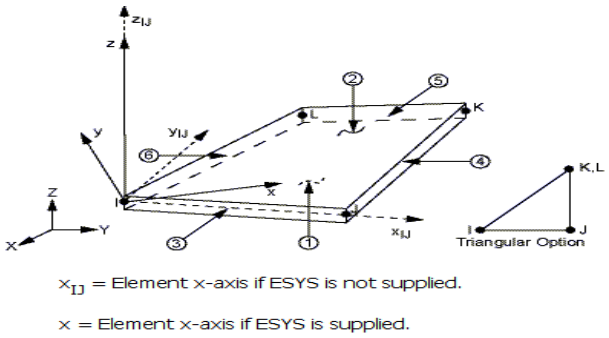

Figure 4-3 Shell41 Geometry (ANSYS, 2012)

SOLID185 is used to model steel plates. It has eight nodes and each node has three degrees of freedom. It is shown in Figure 4-4.

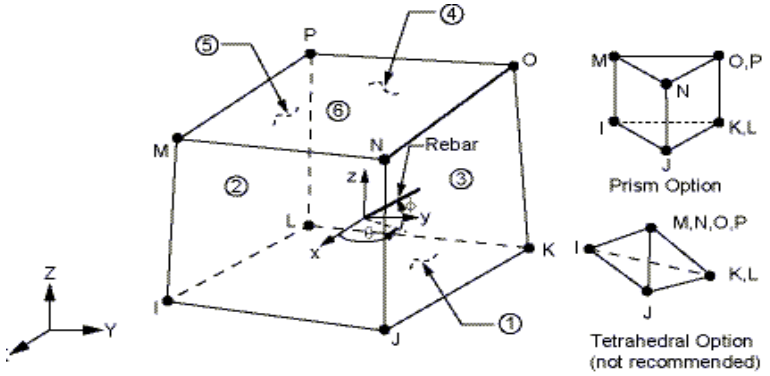

Figure 4-4 Solid185 Homogenous Structural Solid Geometry (ANSYS, 2012)

4.2 Real Constants

Table 4-1 shows the values of real constants that were used in the modeling of the structure. Set 1 represents the low-relaxation grade 270 seven-wire prestressing steel, Set 2 represents #3 mild steel rebars, and Set 3 represents #4 mild steel rebars

Table 4-1 Real Constants

Element	Real Constant		
Link180	Cross-Sectional Area (in.2)	Set 1	0.115
		Set 2	0.110
		Set 3	0.200
Solid65	Material Number	Set 4	0
	Volume Ratio		0
	Orientation Angle		0
Shell41	Thickness (in.)	Set 5	0.04
Solid185	N/A	N/A	N/A

Real Constant Set 4 was used for Solid 65 elements. In this set, material numbers, volume ratio, and orientation angle value are entered as zero to turn off smeared reinforcement capability. In this model, the prestressed girder is modeled using discrete reinforcement.

Real constant Set 5 is used for Shell41 element. Other parameters, such as element x-axis rotation, elastic foundation stiffness, and added mass are entered as zero as they are not applicable for this model.

Real constants are not applicable for Solid185. The initial strain value is given via command prompt as shown below, as there is no direct method available to provide initial strain to the link element (ANSYS, 2012):

!Apply a Constant Strain Of EPEL X=1E-3 For All Girder In A Model

!And Wherever There Is Material=1

inistate,set,dtyp,epel

inistate,set,mat,1

inistate,defi,,,,,0.0063

In the above code, material refers to prestressed steel and 0.0063 is the initial strain provided in each bar.

4.3 Material Properties

All relevant material properties that were used in the modeling are presented in Table 4-2

Table 4-2 Material Properties

Material	Properties		
Prestressed Steel	Linear Isotropic	Elastic Modulus	27.5 x 106 psi
		Poisson's Ratio	0.3
Mild steel rebar	Linear Isotropic	Elastic Modulus	29 x 106 psi
		Poisson's Ratio	0.3
	Bilinear Isotropic	Yield Stress	60 x 103 psi
		Tang Mod	60 x 103 psi
Concrete	Density	Dens	26.9 x 10-4
	Linear Isotopic	Elastic Modulus	5.7 x 106 psi
		Poisson's Ratio	0.25
	Concrete	Open Shear Transfer Coef	0.3
		Closed Shear Transfer Coef	1
		Uniaxial Cracking Stress	750
		Uniaxial Crushing Stress	-1
		Biaxial Crushing Stress	0
		Hydrostatic Pressure	0
		Hydro Biax Crush Stress	0
		Hydro Uniax Crush Stress	0
		Tensile Crack Factor	0

Table 4-2—*Continued*

FRP	*Linear Orthotropic	Elastic Modulus EX	8 x 106 psi
		Elastic Modulus EY	7 x 106psi
		Elastic Modulus EZ	7 x 106psi
		Poisson's Ratio PRXY	0.22
		Poisson's Ratio PRYZ	0.22
		Poisson's Ratio PRXZ	0.30
		Shear Modulus GXY	0.47 x 106 psi
		Shear Modulus GXY	0.47 x 106 psi
		Shear Modulus GXY	0.27 x 106 psi

* (Kachlakev & McCurry, 2000)

Table 4-3 & 4-4 shows mulitilinear isotropic stress-strain properties of steel and concrete.

Strain values are shown in inch/inch and stress values are shown in ksi.

Table 4-3 Multilinear Isotropic Stress-Strain Curve for 270 ksi Strand (Wolanski, 2004)

Stress	Strain	Stress	Strain	Stress	Strain	Stress	Strain
0.0080	220	0.0101	247	0.0121	254	0.0141	258
0.0083	226	0.0103	248	0.0123	255	0.0143	258
0.0085	230	0.0105	249	0.0125	255	0.0145	258
0.0087	233	0.0107	251	0.0127	256	0.0147	259
0.0089	236	0.0109	251	0.0129	256	0.0149	259
0.0091	239	0.0111	251	0.0131	256	0.0151	259
0.0093	241	0.0113	252	0.0133	257	0.0171	260
0.0095	243	0.0115	253	0.0135	257	0.0189	261
0.0097	245	0.0117	253	0.0137	257	0.0215	263
0.0099	249	0.0119	254	0.0139	258	0.301	264

Table 4-4 Multilinear Elasticity for 10 ksi Concrete

Stress	Strain	Stress	Strain	Stress	Strain	Stress	Strain
0.0005	3.0	0.0009	5.0	0.0014	7.0	0.0022	9.0
0.0006	3.5	0.0010	5.5	0.0015	7.5	0.0025	9.5

Table 4-4—*Continued*

0.0007	4.0	0.0011	6.0	0.0017	8.0	0.003	10
0.0008	4.5	0.0013	6.5	0.0019	8.5		

4.4 Modeling

Figure 4-5 shows nodes were created at a certain distance in XY and XZ directions to create the elements. Solid65 and Solid185 elements were created by selecting eight nodes and were copied to fill the entire width and length of the model. Link180 elements were created by connecting the nodes of Solid65 elements. Shell elements were created by connecting the nodes of the Solid65 elements. Link180 and Shell41 elements were directly connected to Solid65 and it created a perfect bond in the concrete model.

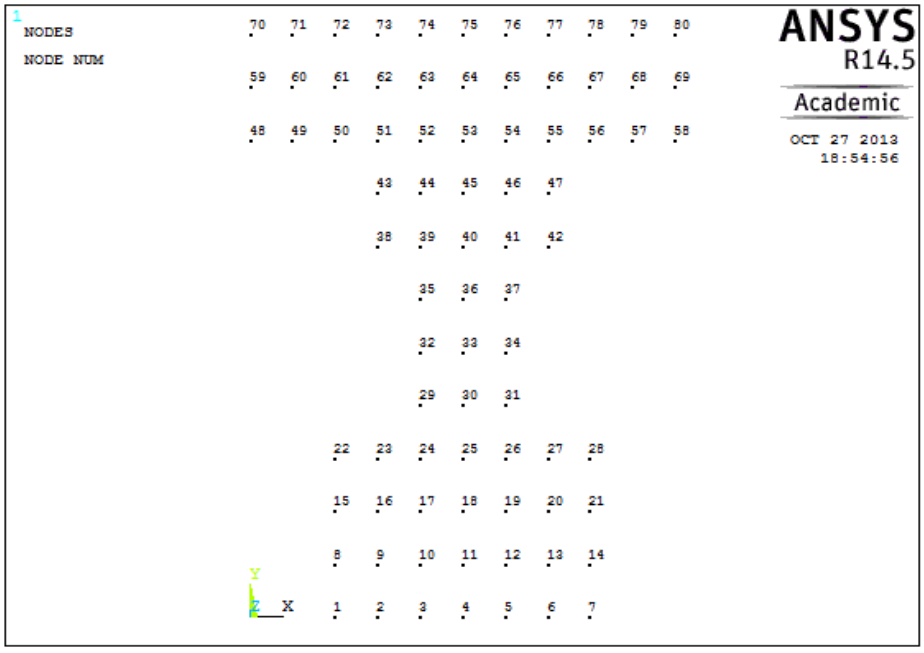

Figure 4-5 Nodes

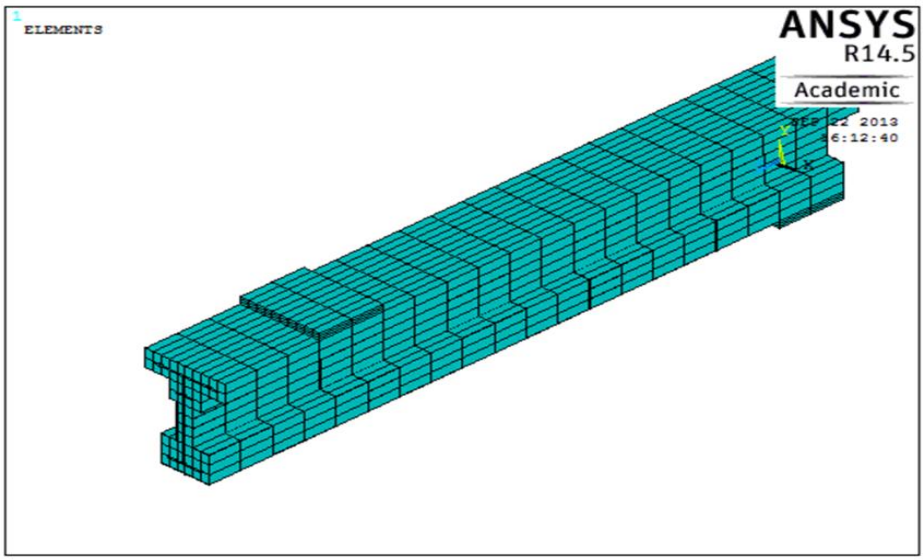

Figure 4-6 Elements Created Using Nodes

Figure 4-6 shows concrete and steel modeled as rectangular element. Element size is modeled uniform throughout for simplicity.

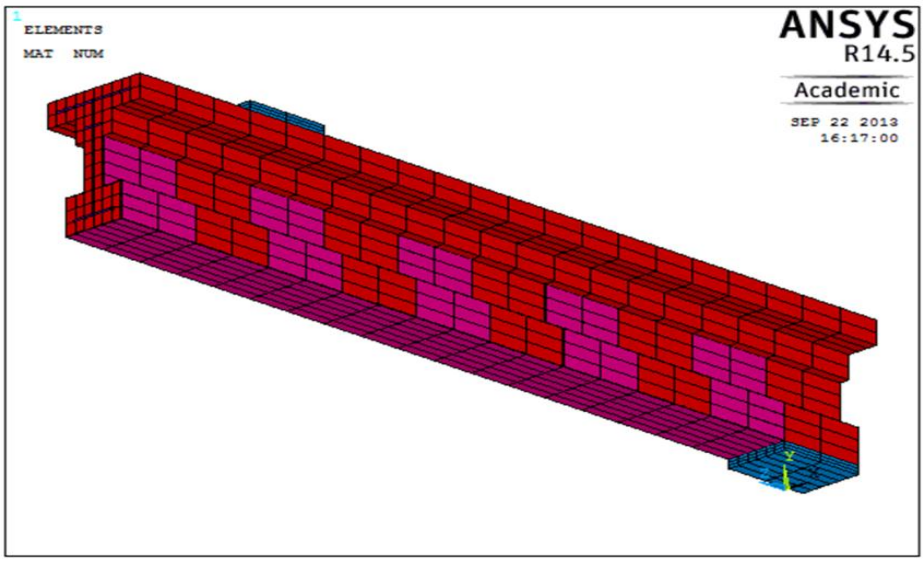

Figure 4-7 3-D View of Model with CFRP Layer

Figure 4-7 shows FRP element applied on top of concrete element. FRP element, shell 45 created by picking concrete element nodes to make perfectly bonded with concrete.

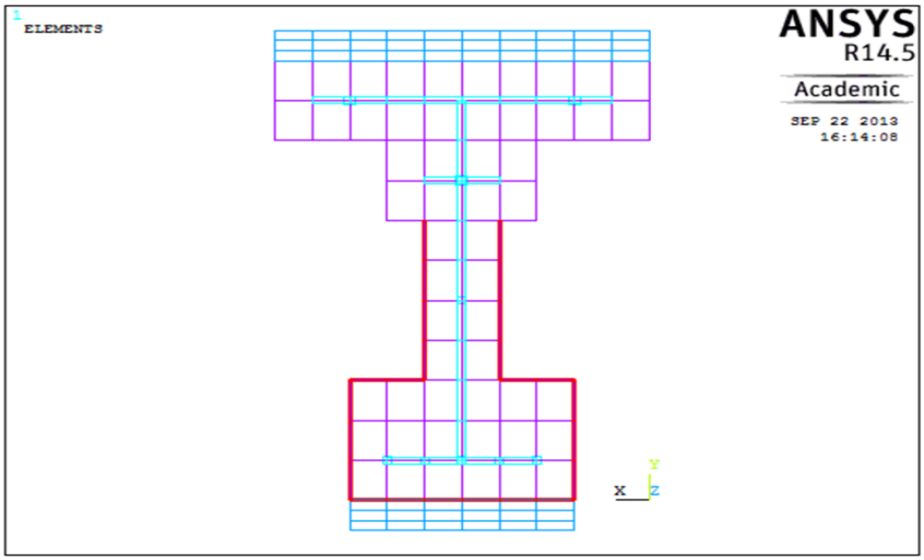

Figure 4-8 Cross-Section View of Model

Figures 4-8 and 4-9 shows cross and longitudinal views of model.

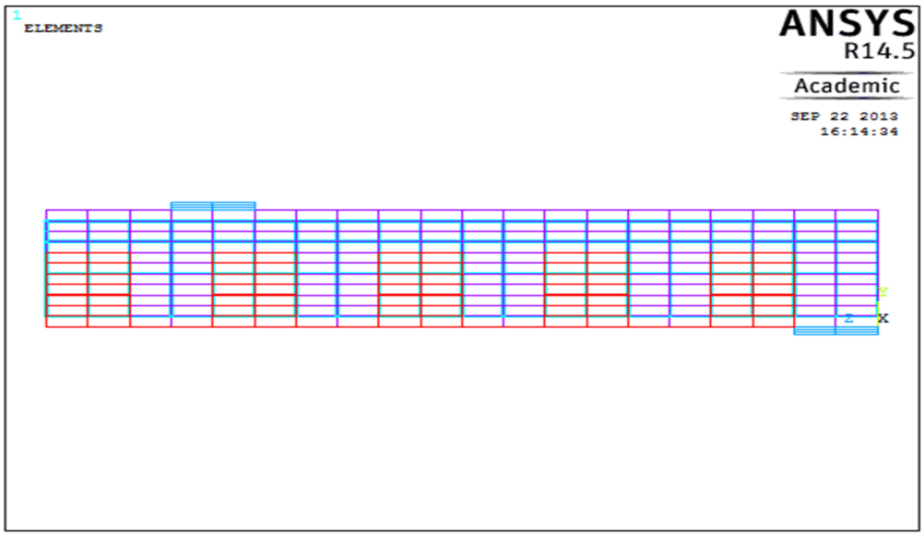

Figure 4-9 Longitudinal View of Model

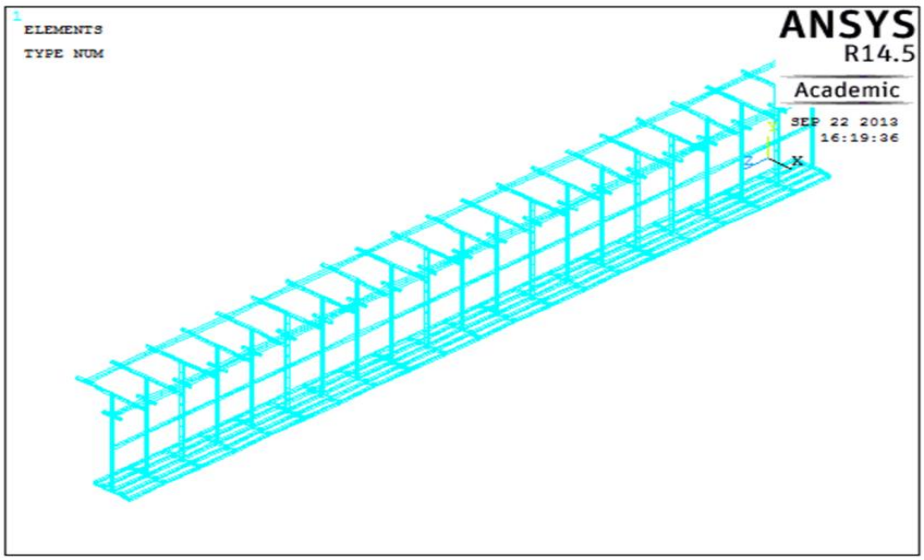

Figure 4-10 Reinforcement Element View

Figure 4-10 shows shear and longitudinal reinforcements are modeled as link element in ANSYS.

4.5 Load and Boundary Condition

Figure 4-11 shows the load and boundary conditions. Using advantage of the symmetric section, only half of the girder was modeled.

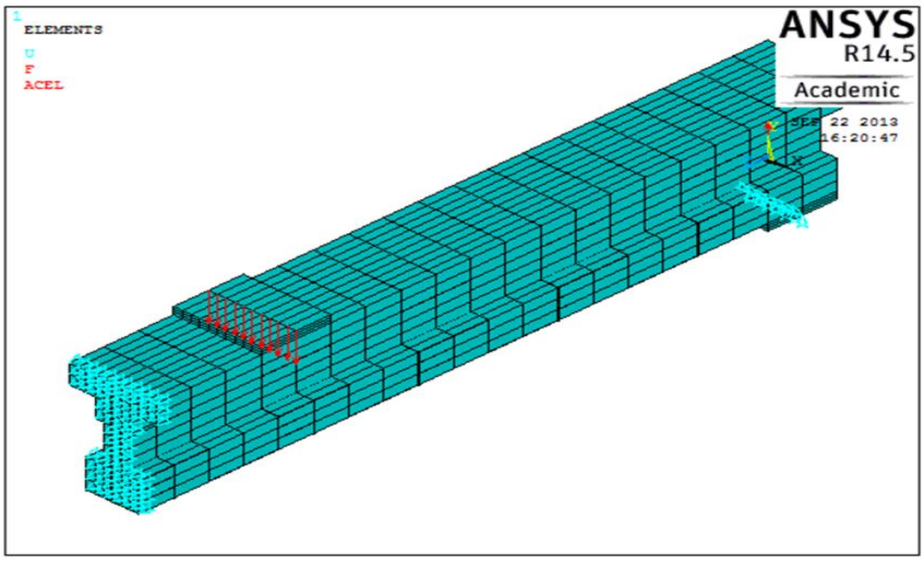

Figure 4-11 Load and Boundary Condition

In Fig. 4-11 left end, the Z direction was constrained to model plane of symmetry. Therefore, the degree of freedom constrain at Z=0 was defined. The roller support modeled provided constraints in the X and Y directions.

4.6 Nonlinear Analysis

The nonlinear analysis was performed to capture the concrete crack pattern from initial stage to failure stage. The load increment was given in a number of steps to achieve convergence in the concrete element. The load increment and the steps are shown in Table 4-3.

Solution control in ANSYS helps to achieve load increment in steps. In this study, small increment static displacements were selected and every step time at the end of loadstep, number of substeps, maximum and minimum number of substeps were entered. It is shown in Figure 4-12. In solution options, sparse direct was selected as default and nonlinear values and limits were given as shown in Fig. 4-13.

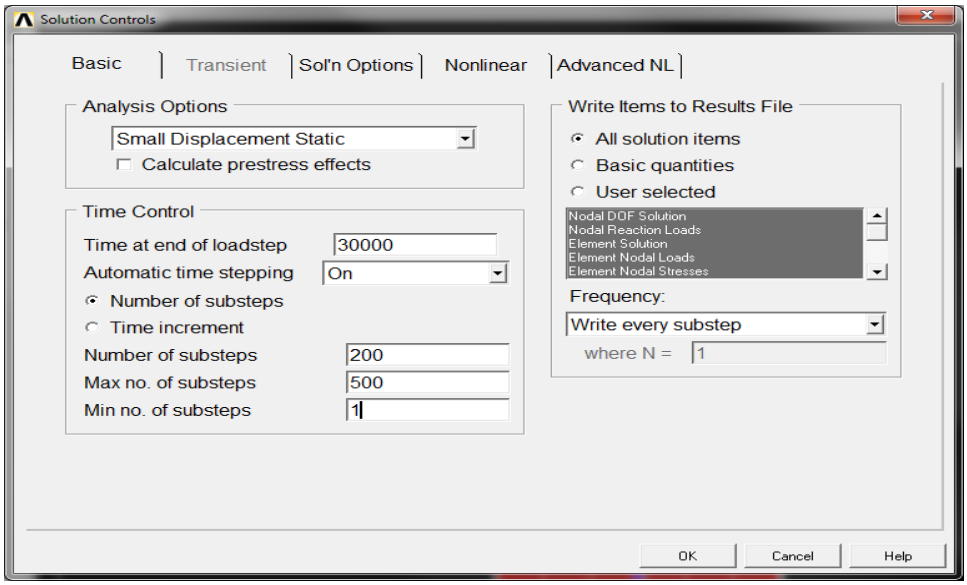

Figure 4-12 Solution Controls

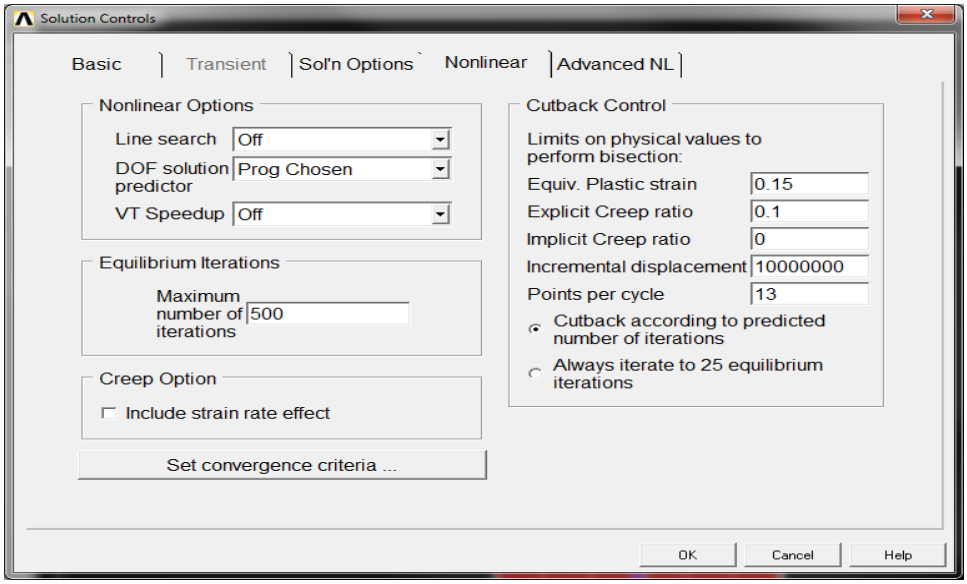

Figure 4-13 Nonlinear Options

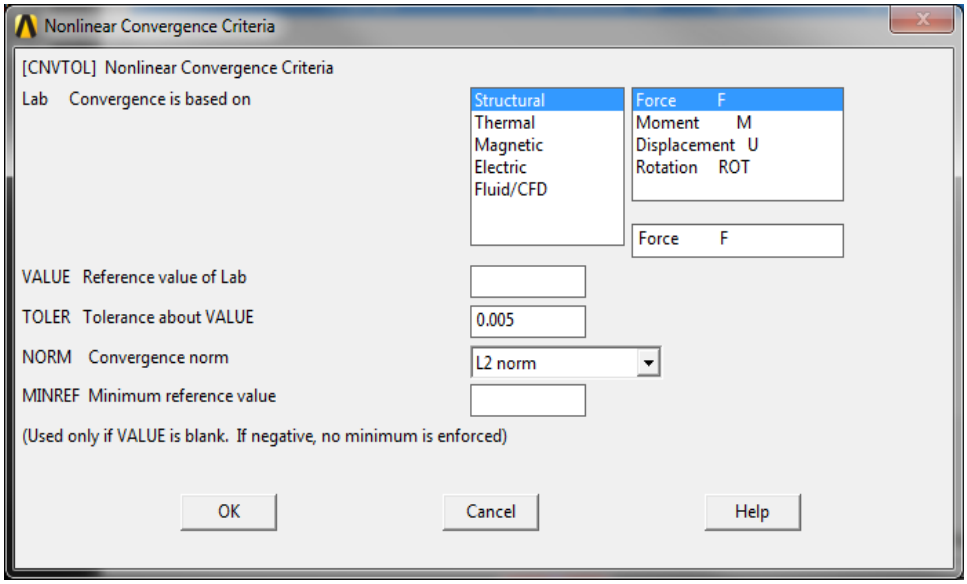

Figure 4-14 Nonlinear Convergence Criteria

Due to convergence problems Force and Displacement tolerances values are given as 0.005 and 0.05. It is shown in Figure 4-14.

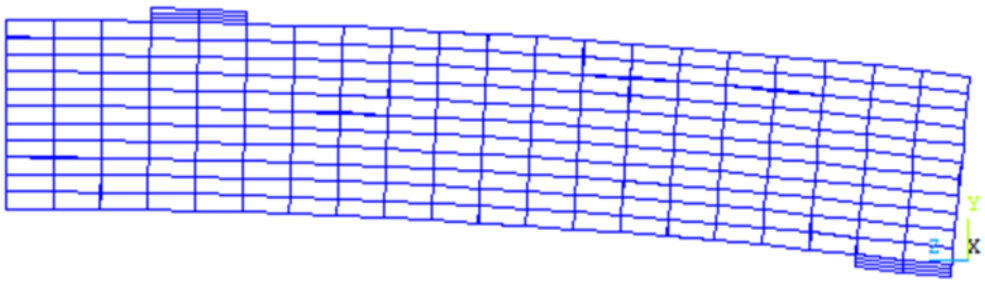

Figure 4-15 Camber Due to Initial Prestress

In the first loadstep, only prestess is provided, and next step gradational force is provided. Figure 4-15 shows camber due to applied initial prestress. Gravitational force automatically calculates self-weight of structure and it produces deflection. After the second loadstep the load is increased constantly until the first crack occurs and steel yields, after that load is gradually decreased until convergence stops.

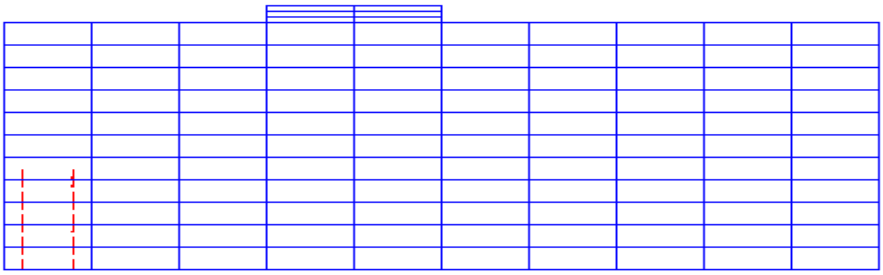

Figure 4-16 Initial Crack

Figure 4-16 shows the initial crack which occurred at step 4 due to the applied load. Figure 4-17 shows the crack pattern at a failure occurred at a step 12.

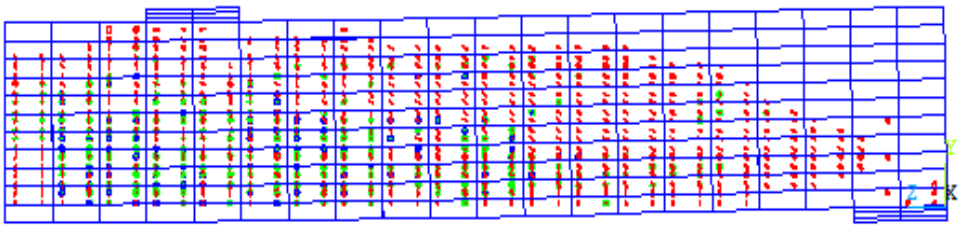

Figure 4-17 Crack Pattern at Failure

4.7 Results and Failure Mode

Table 4-5 shows loadsteps and load increment at a certain time. The model is not converging after step12 due to FRP failure and that is ultimate flexural load capacity of the FRP strengthened model. The final deflection value of 2.178 inches achieved in ANSYS is slightly lower than the experimental value of 2.29 inches. It shows that the ANSYS model is slightly stiffer than experimental model.

Table 4-5 Load Steps

SET	TIME/ FREQ	LOAD STEP	SUB STEP	LOAD in lbs	ANSYS Deflection in inches	Experiment Deflection in inches
1	1	1	1	PRESTRESS	-0.231	-
2	2	2	1	386(GRAVITY)	-0.220	-
3	500	3	4	5,500	0.080	-
4	1,000	4	40	11,000	0.346	-
5	2,000	5	69	16,500	0.587	-
6	2,500	6	155	22,000	1.242	-
7	5,000	7	13	27,500	1.863	-
8	6,000	8	77	14,000	2.049	-
9	7,000	9	69	7,000	2.127	-
10	23,437	10	95	1,000	2.173	-
11	80,418	11	158	100	2.178	-
12	145,265*	12	384	50	2.178	2.29
Total Load in lbs				104,886**		

*Time at failure of prestressed girder

**Total flexural load carrying capacity of prestressed girder.

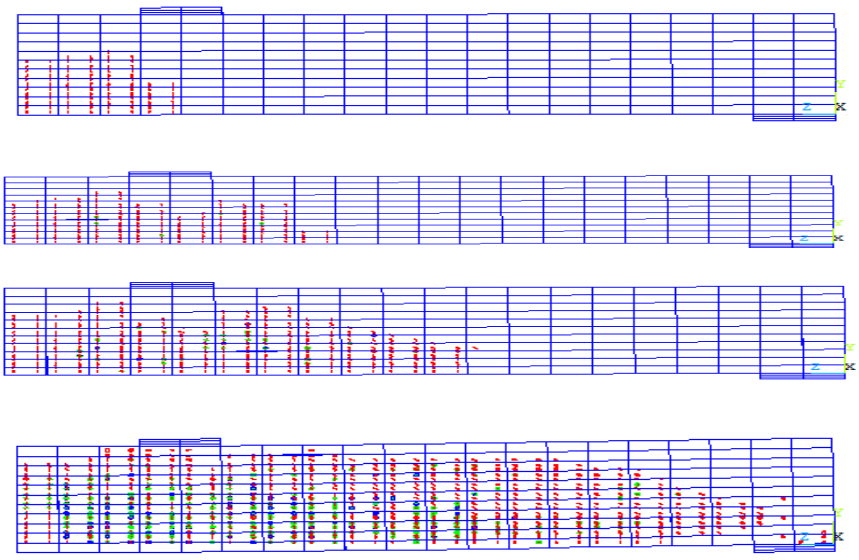

Figure 4-18 Crack Pattern Variation Due to Load Increment

Figure 4-18 shows crack pattern at various stages and load increment.

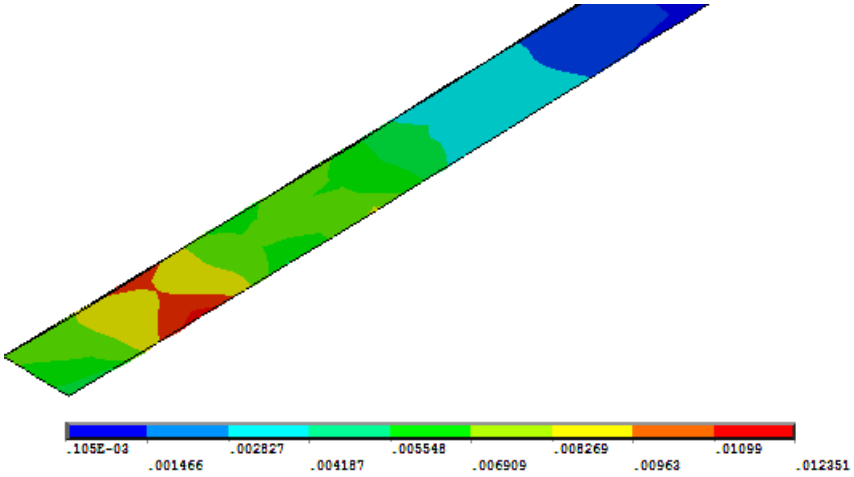

Figure 4-19 Strain Distribution at the Time of Failure

Figure 4-19 shows the strain value in the FRP laminate at the time of failure. The maximum rupture strain of FRP used in this experiment is 0.0120. ANSYS model failed to converge after it achieved a strain value of 0.0123. From the crack pattern and the above figure, it is clear that the ANSYS model has failed in flexure due to FRP rupture.

4.8 Deflection Due To Prestress and Self-Weight

The ANSYS model has been validated by comparing it to the deflection values determined by hand calculation. Both the values are close to each other. The ANSYS value is slightly less than that achieved via hand calculation. Table 4-6 shows deflection due to prestress and self-weight.

Table 4-6 Deflection

.	ANSYS	HAND CALCULATION
Deflection due to prestress (in.)	-0.231	-0.235
Deflection due to self-weight (in.)	-0.220	-0.224

Chapter 5

Comparison And Discussion

In this study ANSYS simulation of FRP flexural strengthened load capacity values were validated based on an experimental study conducted at the University of North Florida and available codes.

Table 5-1 Load Carrying Capacity of FRP flexural Strengthened Girder

	Load Capacity (Kips.)	% Difference	Failure mode
Experimental	99.6*	-	FRP Rupture
ACI	88.5	-11.0	FRP Rupture
AASHTO	106.0	+6.4	FRP Rupture
FIB	85.08	-14.5	FRP Rupture
ISIS	104.0	+4.4	FRP Rupture
TR	86.4	-13.2	FRP Rupture
Mbrace	103.0	+3.4	FRP Rupture
CNR	86.12	-13.5	FRP Rupture
ANSYS	104.9	+5.3	FRP Rupture

*Percentage difference compare to Experimental load capacity

Table 4-1 shows the theoretical Load Capacities achieved using the various code, experiment, and ANSYS model. The stress diagram varies from code to code, and this results in minor variations in load carrying values. Other reasons for this variation in load capacities are due to calculation of moment arm and partial safety factors. The experimental process produced a load capacity of 99.6 kips. The ANSYS simulation of the process gives a simulated load capacity of 104.9 kips. The difference between experimental process and ANSYS simulation is 5%. The reason is that ANSYS model has been designed with the assumption of perfect bonding between concrete and steel, and achieving a perfect bond in experiment is not possible. Another reason for the disparity is the size of the mesh used in the ANSYS model. A smaller mesh size than the

one used in the ANSYS model will give a more accurate value. Experimental and ANSYS simulation values are either higher or lower than the Codal load capacity. The reason is that all codes are considering different material safety factors and environmental safety factors. All the codes, experimental, and ANSYS model predicts FRP rupture failure. The average of all codal failure load predictions is 94 kips, lower than the experimental value. It appears that the average codal prediction is quite conservative. Only the AASHTO and the Mbrace specifications are in line with the theoretical and experimental results for the girder moment capacity. The AASHTO code does not explain much about the FRP strengthening and failure modes, for additional details it refers to the NCHRP reports. Mbrace has discontinued their publication for FRP strengthening and it is recommending ACI 440. ISIS Canada, FIB14, and CNR have published their first edition in initial stage and needs to update based on recent research results. TR 55 second edition in 2012 and ACI 440 2R-08 are developed recently and considering all design and safety parameters.

5.1 Limitations

In the previous experiment, a total of nine girders were tested. Of the nine girders only one girder has been modeled in this study. The model assumed a perfect bond between the concrete and FRP. The epoxy layer present in between the FRP and concrete has not been modeled in this study, due to the assumption made that there exists a perfect bond between the concrete and FRP. All the codes considered in this study provide procedures for flexural, shear, and axial strengthening. This study has been limited to investigation of flexural failure due to FRP rupture only.

Chapter 6

Conclusions

- A number of design codes, standards and guidelines are available worldwide that deal with FRP strengthening of concrete structures. They present equations for the prediction of flexural, shear, axial and torsional strengths of such strengthened structures. Some of these documents contain different stress distributions for the flexural strength determination and it results variation in load capacity prediction.
- The maximum flexural load capacity is obtained through the AASHTO 2012 code, and the minimum through FIB code. However, the variations in load capacities are moderate (maximum 14%).
- Experimental results have been validated with Finite Element analysis and the difference between experimental value and FEM value is around 5%.
- Experimental, codes and ANSYS simulations all predict flexure failure initiated due to FRP rupture.
- ANSYS 14.5 is capable of predicting crack patterns and failure modes in the FRP girders.
- Various design standards are quite conservative in predicting the flexural capacity of a FRP strengthened AASHTO girder.
- It is recommended that the AASHTO guidelines be followed for designing FRP strengthening systems for concrete bridges. The MBrace guidelines have been discontinued by the publishers. The AASHTO guidelines are reasonable and predict strength values that are consistent with the theoretical modeling and also experimental results.

- In this study, only flexural capacity of the strengthened girder was considered. Other parameters, such as shear, torsion and deflection, were not considered. It should be noted that the design codes contain provisions for the calculation of most of these parameters. The experimental study considered herein was focused only on flexural strengths.

6.1 Future Research Recommendations

The above research can be extended as follows:

- Prestress losses in FRP strengthened girder has not been investigated in this study. It needs to be investigated further to get a more accurate FRP strength value.
- This study has been performed using mesh size of 1.5 x 2 x 6 inch. A smaller mesh size would yield a more accurate flexural strength from the simulation.
- FRP rupture failure mode was investigated in this study. Other modes of failure also need to be investigated.
- Flexural strength of the girder has been investigated in this study as recommended by various codes. Shear, axial, and torsional strengthens of various codes also need to be investigated.
- The study has been performed with the assumption that a perfect bonding exists between the concrete and FRP. However, the strength of the girder needs to be investigated taking the epoxy layer present between the concrete and FRP into consideration.

Appendix A

Finite Element Modeling Procedure

Click on the Start Menu and point to ANSYS Mechanical APDL. A window as shown below will appear prompting you to enter several input parameters for the simulation that we intend to do with ANSYS Mechanical APDL .

START →ANSYS Mechanical APDL →PREFERENCES →SELECT STRUCTURAL

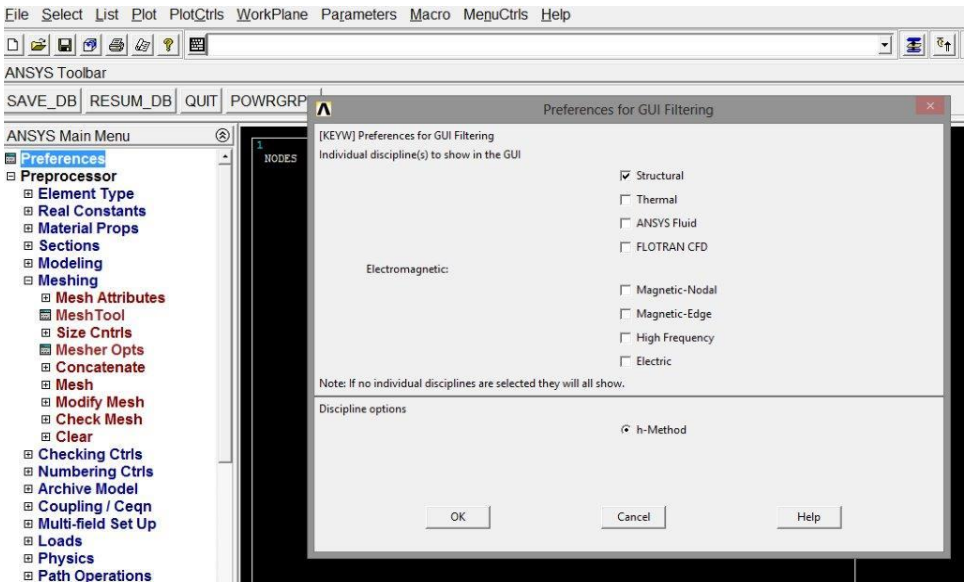

Creating Geometry

In order to create any object , you have to define all of the keypoints for that object. To create a keypoint , click on the Active CS . A window will appearsprompting you to enter the keypoint number and its coordinates

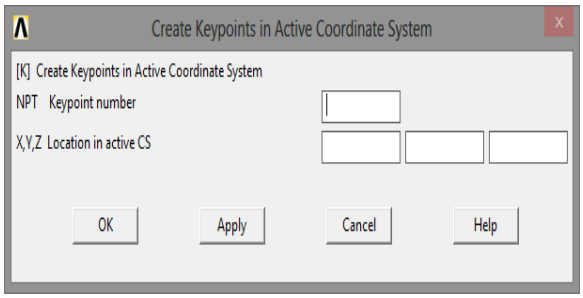

To create a Line , click on the line icon, a window will appear which will ask you to pick the key points . Based on the dimensions , the lines elements for the model is given below

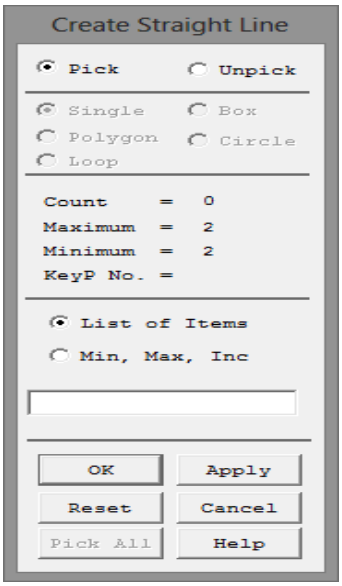

To create the AREA fillet , select the lines that forms the area and click apply

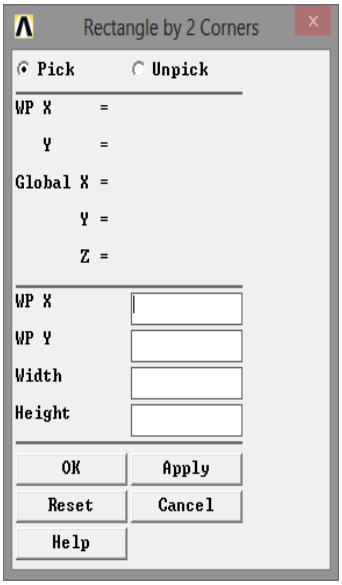

Now to create a block volume , as per the model dimensions , click on the volume (Modeling→create →volume), a window will appear which will ask for the areas to extrude .

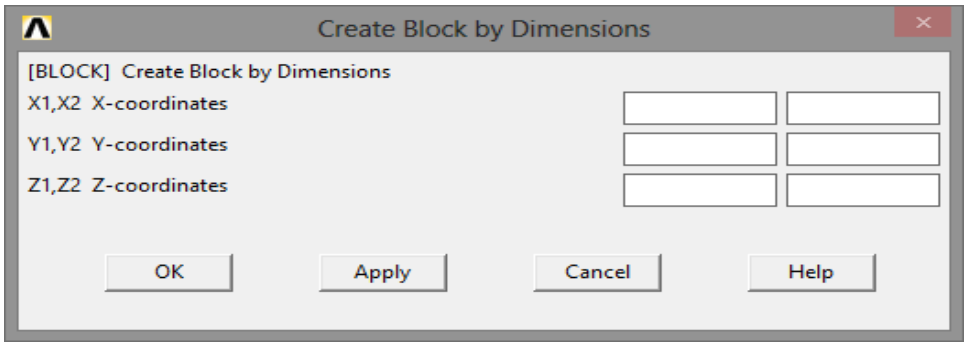

After the creation of the model, you should define the steel reinforcement via 3 parameters

Elements Types

In the ANSYS main menu , select Preprocessor →Element type , click add , a window will appear asking you to define the elements . Select the elements

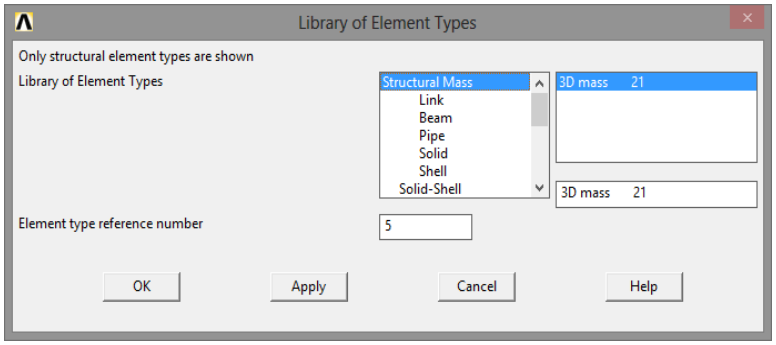

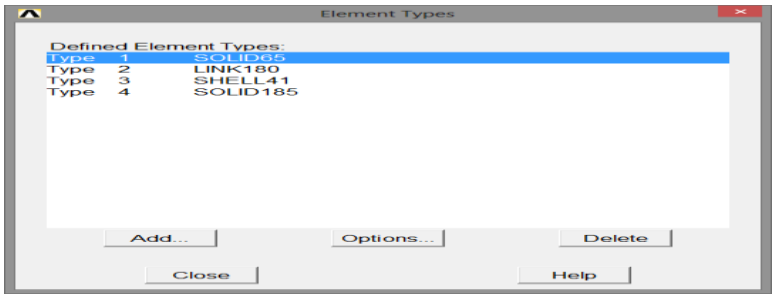

Real Constants

In the Preprocessor menu , select Real constant and click add. A window will appear which will ask you to define the constant sets.

Then a window will appear after clicking add , select the element types

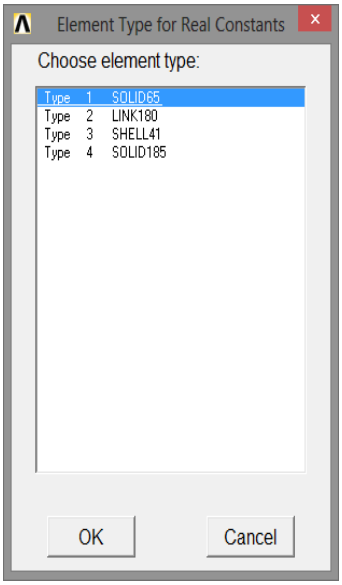

Select the set of real constants and edit the constants by clicking “edit ” in the previous dialogue box . Make sure to select the set before clicking edit button .

Real Constant for SOLID 65

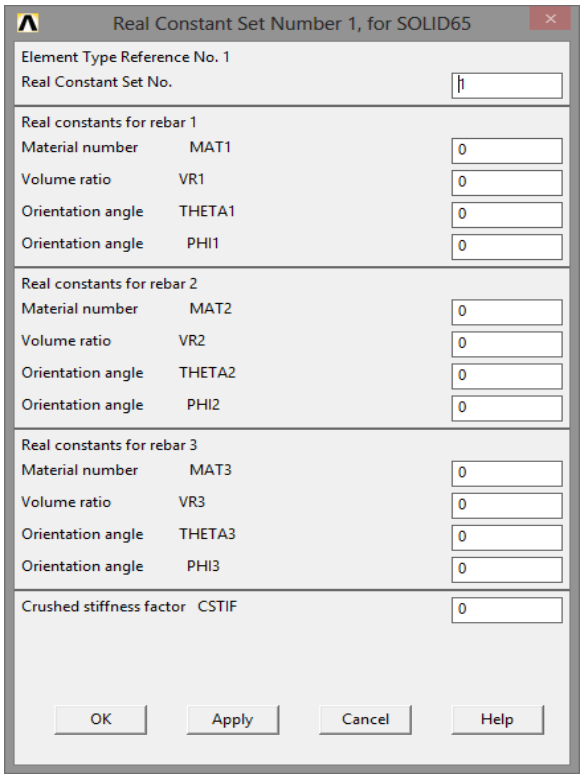

Real constant for LINK180

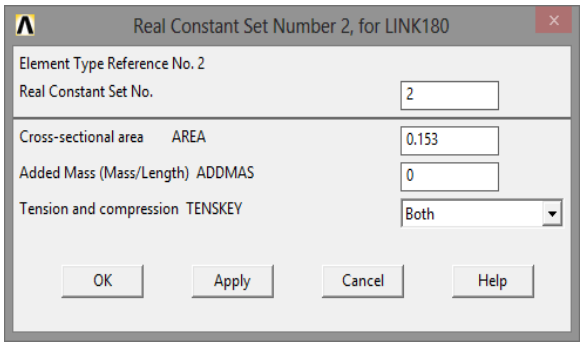

Material Properties

Define “Material Properties” as follow: click on “Material Models” under “Material Props” as shown highlighted below.

Linear elastic Isotropic – Steel

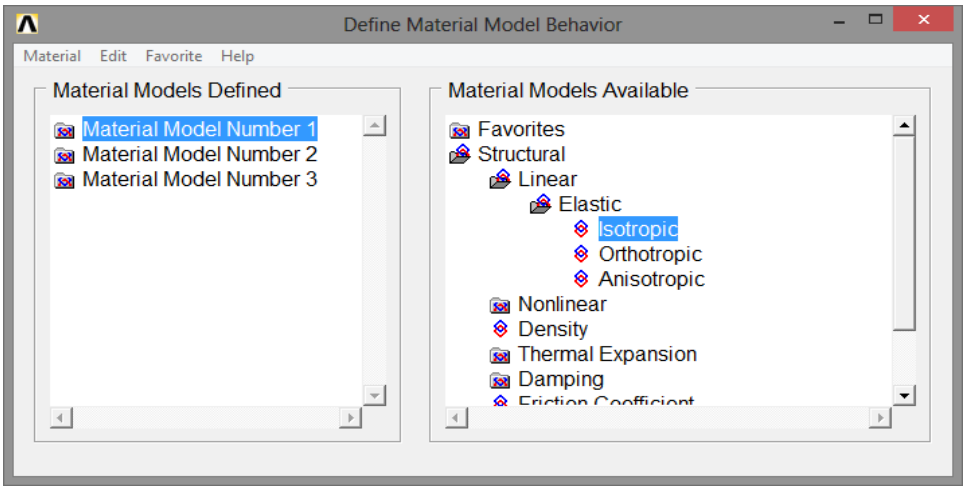

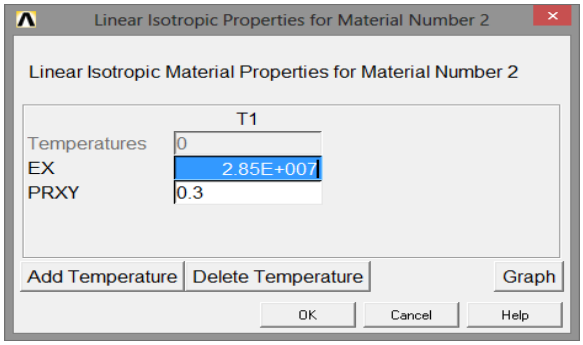

Orthotropic - Fiber Reinforced Polymer

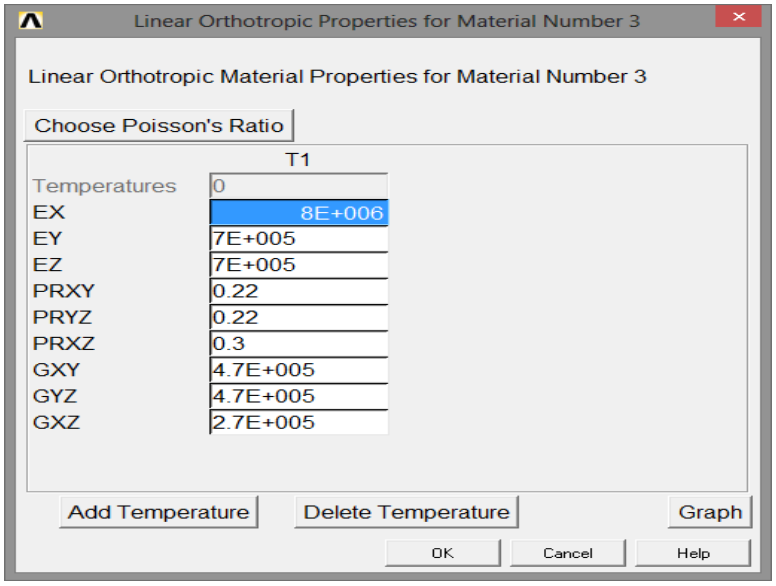

Non linear –> inelastic –> non metal plasticity –> concrete

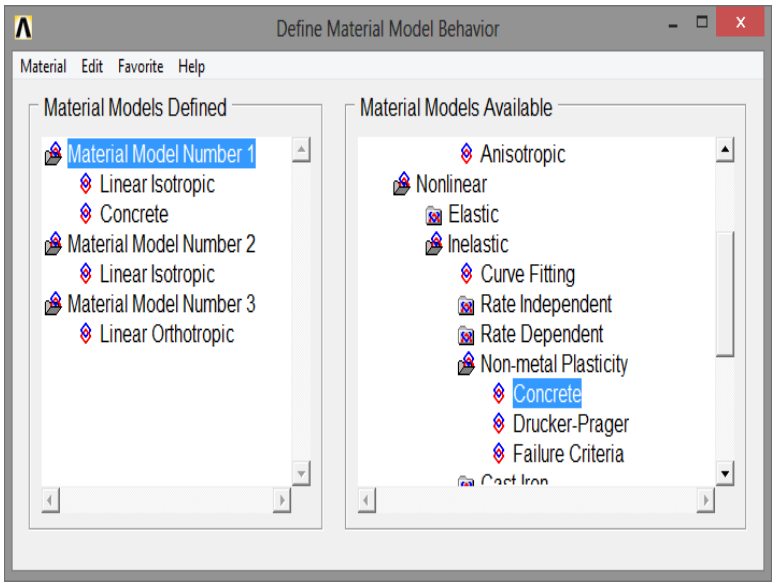

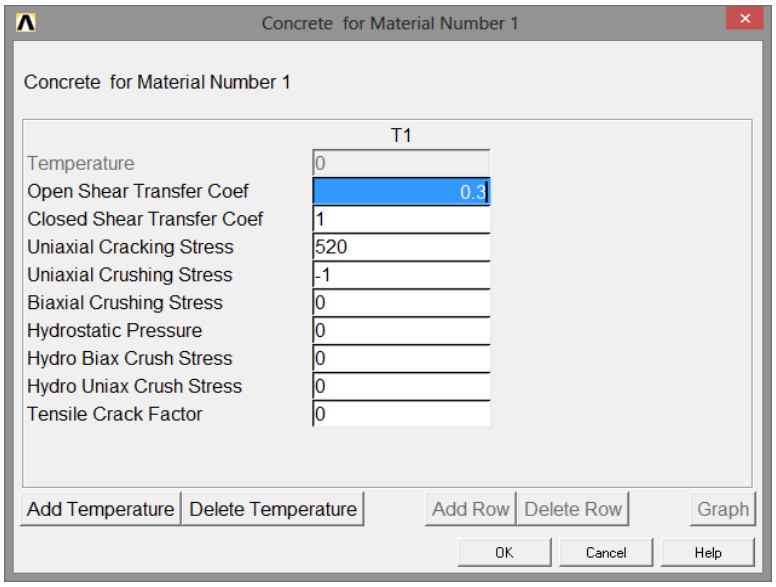

Now after defining the material properties, the model is converted into a form to carry out finite element simulation.

From the ANSYS Main Menu , select Meshing →Mesh attributes . This process will allow you to assign the material properties to appropriate element for doing finite element analysis .

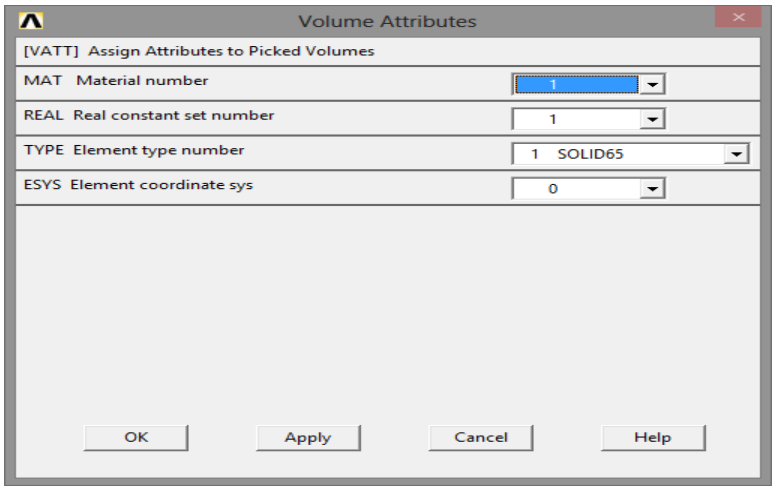

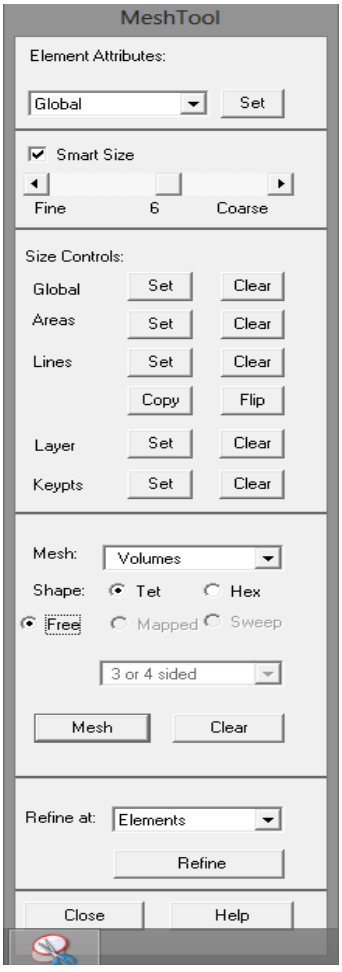

Now after meshing , define the loads to carry out the simulation .

Preprocessors →Loads →Analysis Type → New analysis

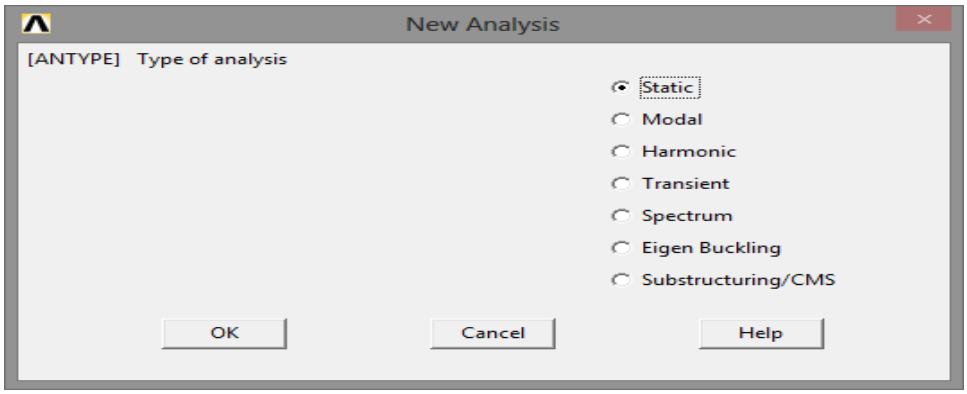

Then define the loads by Preprocessors →Loads →Define Loads → Apply → Structural → Displacement→Lines (to define the boundary conditions)

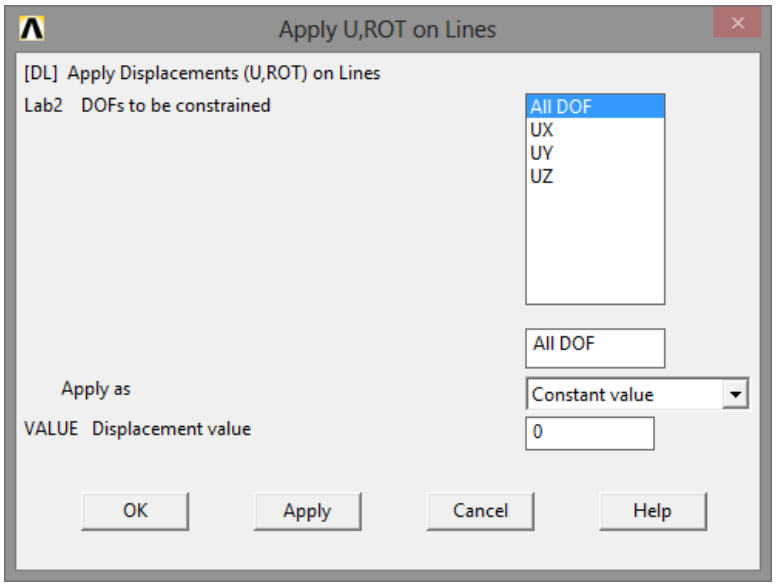

(For Simply Supported , Displacement Value =0)

Now define the uniformly distributed load by Preprocessors →Loads →Define Loads → Apply → Structural → Pressure→ on areas and Pick the areas

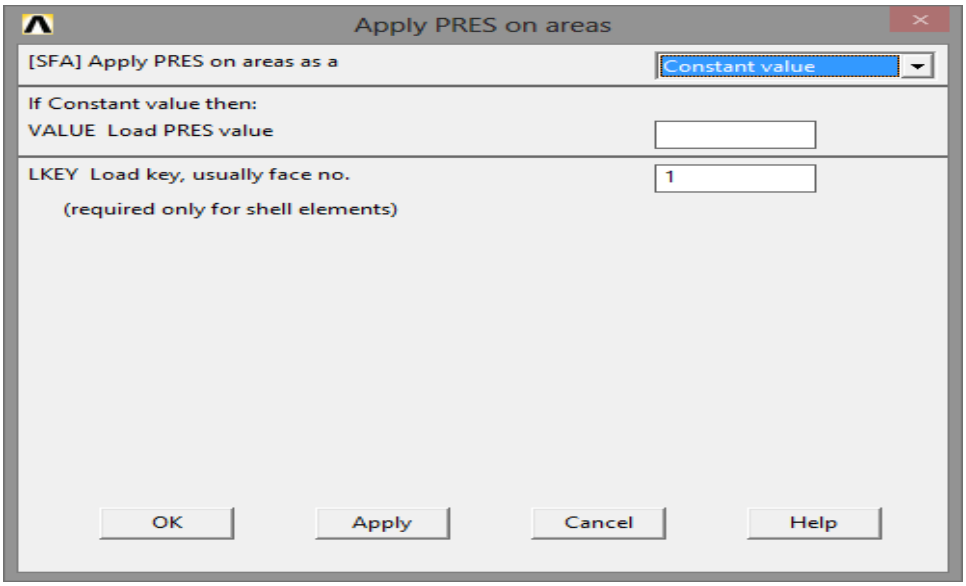

Now Solution→Solve→ current LS

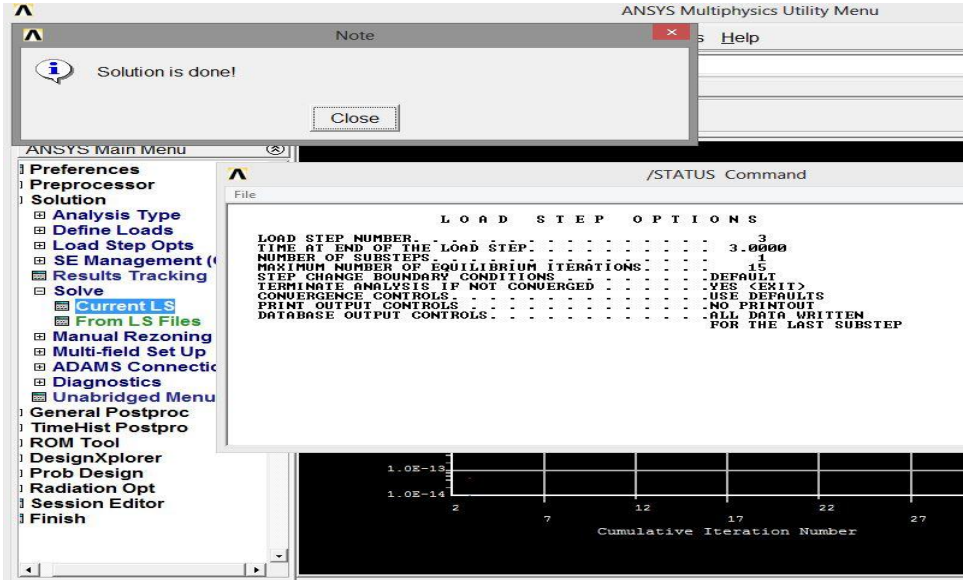

Appendix B

Notations

A_f - Area of FRP external reinforcement, $in.^2$

A_{ps} - Area of pre-stressed reinforcement in tension zone, $in.^2$

b - Width of compression face of member, in.

c - Distance from extreme comp. fiber to the neutral axis, in.

d_{ps} - Distance from extreme compression fiber to centroid of prestressed reinforcement, in.

E_f - Tensile modulus of elasticity of FRP, psi

f_{cd} - Design concrete compressive strength, psi

f_{fe} - Effective stress in the FRP; stress level attained at section failure, psi

f_{ps} - Stress in prestressed reinforcement at nominal strength, psi

h - Overall thickness or height of a member, in.

k_2 - Multiplier for locating resultant of the compression force in the concrete

M_r - Factored moment capacity of the section, k-ft

β_1 - Ratio of depth of equivalent rectangular stress block to depth of the neutral axis for concrete

γ_{Rd} - Partial factor for resistance models.

ε_c - Strain level in top surface of concrete, in./in.

ε'_c - Maximum strain of unconfined concrete corresponding to f'_c in/in.

ε_{fe} - Effective strain level in FRP reinforcement attained at failure, in/in. .

ε_o - the concrete strain (in/in) corresponding to the maximum stress of the concrete stress-strain curve

λ - Resultant of the compression stress

σ_f - Stress in FRP reinforcement

Φ - Resistance factor

Φ_f - FRP resistance factor

Ψ - Resultant of the compression stress.

Appendix C

Hand Calculation

Deflection Due to Prestress:

Initial Prestress	(F_i)	= 99,475 lbs.
Initial Elastic Modulus	(E_{ci})	= 5.13 x 10^6 psi
Gross Moment of Inertia	(I_g)	= 8,070.31 in^4
Clear Span	(l)	= 228 in.
Weight of Girder	(w_g)	= 12.83 lbs.
Eccentricity from Netural axis to CG of Prestress Strand	(e)	= 15.1 in.

$$\Delta_{fi} = -\frac{F_i l^2}{8\, E_{ci} I_g}(e)$$

= -0.235 inch.

Deflection due to Prestress and Self Weight:

$$\Delta_{fi} + \Delta_g = -\frac{F_i l^2}{8\, E_{ci} I_g}(e) + \frac{5\, w_g l^4}{384 E_{ci} I_g}$$

= -0.235 + 0.011

= -0.224 inch.

References

AASHTO. (2012). *Guide Specifications for Design of Bonded FRP Systems for Repair and Strengthening of Concrete Bridge Elements* (1st ed.). Washington, DC: American Association of State Highway and Transportation Officials.

ACI. (2008). *440.2R-08 Guide for the Design and Construction of Externally Bonded FRP Systems for Strengthening Concrete Structures*. Michigan: American Concrete Institute.

ANSYS. (2012). ANSYS Parametric Design Language (Version 14.5). Canonsburg, Pennsylvania: ANSYS.

CNR-DT 200. (2004). *Guide for the Design and Construction of Externally Bonded FRP Systems for Strengthening Existing Structures*. Rome, Italy: Italian Advisory Committee on Technical Recommendations for Construction.

ElSafty, A., & Graeff, M. K. (2012). The Repair of Damaged Bridge Girders with Carbon Fiber Reinforced Polymer “CFRP” Laminates. Retrieved from http://trid.trb.org/view.aspx?id=1224031

FIB Bulletin 14. (2001). *Externally Bonded FRP Reinforcement for RC Structures*. Europe: The International Federation for Structural Concrete.

GangaRao, H., & Vijay, P. (1998). Bending Behavior of Concrete Beams Wrapped with Carbon Fabric. *Journal of Structural Engineering*, *124*(1), 3–10. doi:10.1061/(ASCE)0733-9445(1998)124:1(3)

Gilstrap, J. M., Burke, C. R., Dowden, D. M., & Dolan, C. W. (1997). Development of FRP reinforcement guidelines for prestressed concrete structures. *Journal of Composites for Construction*, *1*(4), 131–139.

ISIS. (2001). *Strengthening Reinforced Concrete Structures with Externally-bonded Fiber-reinforced Polymers*. Winnipeg, Manitoba: ISIS Canada Design Manuals.

Kachlakev, D., & McCurry, D. D. (2000). Behavior of full-scale reinforced concrete beams retrofitted for shear and flexural with FRP laminates. *Composites Part B: Engineering*, *31*(6–7), 445–452. doi:10.1016/S1359-8368(00)00023-8

Miller, A. D. (2006). Repair of Impact-Damaged Prestressed Concrete Bridge Girders Using Carbon Fiber Reinforced Polymer (CFRP) Materials. Retrieved from http://repository.lib.ncsu.edu/ir/handle/1840.16/752

NCHRP Report 655. (2010). *Recommended Guide Specification for the Design of Externally Bonded FRP Systems for Repair and Strengthening of Concrete Bridge Elements*. National Cooperative Highway Research Program.

Report Card on America's Infrastructure. (2013). *Infrastructurereportcard.org*. Retrieved from http://www.infrastructurereportcard.org/bridges/

Tedesco, J. W., Stallings, J. M., & EL-Mihilmy, M. (1998). Rehabilitation of a reinforced concrete bridge using FRP laminates. *Final Report*, 930–341.

TR55. (2012). *Design Guidance for Strengthening Concrete Structures Using Fiber Composite Materials* (3rd ed.). Surrey, United Kingdom: The Concrete Society.

U.S department of transportation federal highway administration. (2012). *fhwa.dot.gov*. Retrieved from http://www.fhwa.dot.gov/bridge/nbi.cfm

Wolanski, A. J. (2004). *Flexural behavior of reinforced and prestressed concrete beams using finite element analysis*. Faculty of the Graduate School, Marquette University. Retrieved from http://www.eng.mu.edu/foleyc/MS_Theses/wolanski_2004_MS.pdf

Yang, D., Merrill, B. D., & Bradberry, T. E. (2011). Texas' Use of CFRP to Repair Concrete Bridges. *ACI Special Publication*, *277*.

Biographical Information

Muruganandam Mohanamurthy received his B.E in Civil Engineering from Anna University, India in 2009. He started his career as a graduate engineer at Larsen & Toubro, Construction Company, India from 2009 to 2011. During this period he worked as a senior engineer for apartment building construction. His work mainly included assisting structural design engineer and preparing schedules. He joined University of Texas at Arlington as a graduate student in the Civil Engineering Department in 2011. He started his thesis research under Dr. Nur Yazdani in the application of fiber reinforced polymer for bridge strengthening.